Available online at www.sciencedirect.com

ScienceDirect

Ceramics International 40 (2014) 993–1000

CERAMICS INTERNATIONAL

www.elsevier.com/locate/ceramint

Double layer bioglass-silica coatings on 316L stainless steel by sol–gel method

S. Pourhashem, A. Afshar*

Department of Materials Science and Engineering, Sharif University of Technology, Azadi Avenue, P.O. Box 11155-9466 Tehran, Iran

Received 27 February 2013; received in revised form 23 May 2013; accepted 21 June 2013
Available online 1 July 2013

Abstract

The application of bioglass coatings on metallic implants provides link between bone and materials and prevents corrosion of metallic implants in body fluid. Therefore, in this research, 45S5 bioglass-silica coatings on 316L stainless steel were prepared by the sol–gel method and were characterized by different techniques. According to X-ray diffraction (XRD) results, by sintering 45S5 bioglass at 600 °C for 5 h, coatings containing both amorphous phase and $Na_2Ca_2Si_3O_9$ crystalline phase were obtained. Scanning electron microscopy (SEM) results showed that coatings prepared via appropriate sol aging and substrate preparations are crack-free. Potentiodynamic polarization tests in simulated body fluid (SBF) showed that coatings improve corrosion resistance of substrates, significantly. Further, bioactivity was considered during 30 days of immersion in SBF at 37 °C by atomic absorption spectroscopy (AAS), XRD, SEM and potentiodynamic polarization tests that demonstrated the growth of amorphous apatite, hydroxyapatite (HA) and $CaSiO_3$ film on coatings.

Keywords: C. Corrosion; Bioglass; SiO_2; Coating; 316L stainless steel; Sol–gel

1. Introduction

316L Stainless steel is biocompatible and has been used for many decades as a permanent surgical implant material due to its lower cost, excellent fabrication properties, good corrosion resistance, and easy availability [1,2]. However, the corrosion of the metallic implants in physiological solutions is critical because it could affect negatively the biocompatibility and the mechanical integrity [3]. Large concentrations of metallic cations coming from the prosthesis can result in biologically adverse reactions and might lead to the mechanical failure of the implant [1,3].

On the other hand, bioactive glasses are defined by Hench [4] as materials capable to create a chemical bond with surrounding tissues which leads to an intimate link between bone and materials [5]. Bioactive glasses exhibit osteoinductive behavior, are able to bond to soft and hard tissues and form a carbonated hydroxyapatite layer on their surface with composition and structure equivalent to the mineral phase of bone when exposed to biological fluid [4,6]. Although bioactive glasses have been used clinically as bone regenerative materials in dental and orthopedic applications [7], these materials are normally very brittle and prone to crack propagation leading to catastrophic failure [8]. Hence, due to their limited mechanical properties, they cannot be used as a bulk material in load-bearing applications [9,10].

Therefore, in order to use the excellent bioactivity of the bioactive glasses, as well as the advantageous mechanical properties of metals, the bioactive coated implants are good options to overcome mentioned limitations [8,11]. Although there are various ways to apply bioactive glasses as coatings on metal implants such as sol–gel [12], plasma spraying [13] and electrophoretic deposition [14], the sol–gel process offers a number of advantages over other coating methods like flexibility, control of coating morphology, chemistry and structure [15].

In previous studies, SiO_2–CaO–P_2O_5 bioglass were used to prepare one layer bioglass coating via sol–gel method and silica-bioglass coatings were prepared by suspensions containing bioglass particles. In this research, double layer coatings containing silica (SiO_2) intermediate layer and 45S5 bioglass

*Corresponding author. Tel.: +98 21 6616 5204; fax: +98 21 6600 5717.
E-mail address: Afshar@sharif.edu (A. Afshar).

0272-8842/$ - see front matter © 2013 Elsevier Ltd and Techna Group S.r.l. All rights reserved.
http://dx.doi.org/10.1016/j.ceramint.2013.06.096

(SiO_2–CaO–Na_2O–P_2O_5) top layer were prepared by sol-gel procedure on 316L stainless steel substrates. Several approaches have been used to evaluate the characteristics of the prepared coatings such as their phase structure, morphology and corrosion resistance. Besides, the bioactivity of coatings during 30 days of immersion in simulated body fluid (SBF) was considered by different techniques.

2. Experimental

In this research, AISI 316L austenitic stainless steel was used as the substrate material and two different methods were utilized for surface preparation in order to compare their effect on coating properties: (a) mirror polished substrates; (b) substrates sandblasted with silica beads. Besides, some of the sandblasted substrates were treated in acid nitric 25% vol for 12 h. At last, the specimens were ultrasonically cleaned in acetone before the application of coatings.

In order to prepare the silica sol, tetraethyl orthosilicate (TEOS, Merck) was added to ethanol (ethanol:TEOS molar ratio was 5:1) and HCl. Then, distilled water was added to the solution (H_2O: TEOS molar ratio was 4:1) and allowed to mix at room temperature till a clear solution was achieved [16].

45S5 bioglass sol with chemical composition of 45 wt% SiO_2:6 wt% P_2O_5:24.5 wt% Na_2O:24.5 wt% CaO was prepared by sol–gel process [17,18]. Tetraethyl orthosilicate (TEOS, Merck) was added into 0.1 mol/L HNO_3 (Merck) as catalyst at room temperature. The following chemicals were added sequentially and about 1 h was given to each reagent to react thoroughly under stirring: thriethyl phosphate (TEP, Merck), sodium nitrate ($NaNO_3$, Merck) and calcium nitrate tetrahydrate ($Ca(NO_3)_2 \cdot 4H_2O$, Merck), respectively. To allow completion of the hydrolysis reaction and achieving a clear sol, stirring was continued for 1 h after the last addition.

To prepare double layer coatings consisting of an intermediate silica layer and a top 45S5 bioglass layer, at first, the silica coatings were prepared by dipping the substrates into the silica sol aged for 24 h at room temperature and the dip coating withdrawal rate was 5 cm/min, followed by drying silica coated substrates in oven at 110 °C for 30 min and then, heat treated at 450 °C for 30 min in a programmable furnace with heating rate of 1 °C/min. Next, these samples were dip coated in 45S5 bioglass sol aged at 50 °C and the dip coating withdrawal rate was 5 cm/min, followed by drying at room temperature and then, heat treated at 600 °C for 5 h in a programmable furnace with heating rate of 1 °C/min and overall obtained thickness is about 4 μm.

The SS 316 alloy used as substrate is stabilized grade stainless steel (with 0.03 wt% of carbon) and this material is required to be heat treated at 650–675 °C in order to be sensitized, although the most commonly used sensitizing treatment is 1 h at 675 °C. However, for this stainless steel alloy, the sensitizing appears after the 50 h at 650 °C [19]. Therefore, the heat treatment selected in this research seems to have negligible effect on substrate.

Characteristics of synthesized samples were considered by X-ray diffractometer (XRD, Philips Analytical, 40 KV, 30 mA, Cu), scanning electron microscopy (SEM, VEGA, TESCAN), pull-off method (Elcometer, HATA 108) and potentiodynamic polarization tests (Autolab PGSTAT 302N). A three electrode cell with a saturated calomel electrode (SCE), a working electrode (the sample) and a counter electrode (Graphite) was employed in polarization test and scan rate potential was set at 1 mV/s going from the cathodic to the anodic side. The corrosion polarization curves were plotted after 1 h in order to attain steady open circuit potential. Corrosion potential (E_{corr}), corrosion current density (i_{corr}) and the anodic/cathodic

Table 1
Order and amounts of reagents for preparing 1000 ml of SBF.

Order	Reagent	Amount
1	NaCl	8.035 g
2	$NaHCO_3$	0.355 g
3	KCl	0.225 g
4	$K_2HPO_4.3H_2O$	0.231 g
5	$MgCl_2.6H_2O$	0.311 g
6	1.0 M HCL	39 ml
7	$CaCl_2$	0.292 g
8	Na_2SO_4	0.072 g
9	Tris	6.118 g
10	1.0 M HCl	0–5 ml

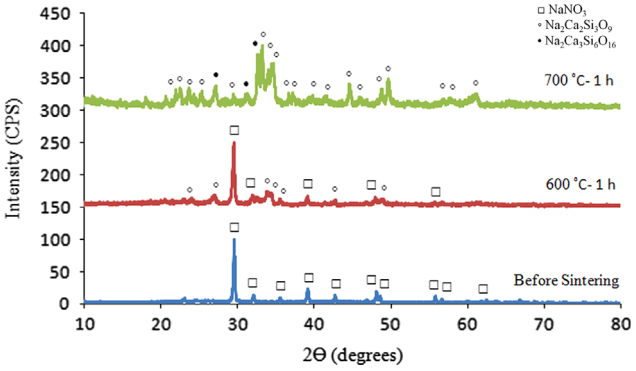

Fig. 1. XRD pattern of 45S5 bioglass before sintering and after sintering at 600 and 700 °C for 1 h (□ $NaNO_3$, ◦ $Na_2Ca_2Si_3O_9$, • $Na_2Ca_3Si_6O_{16}$).

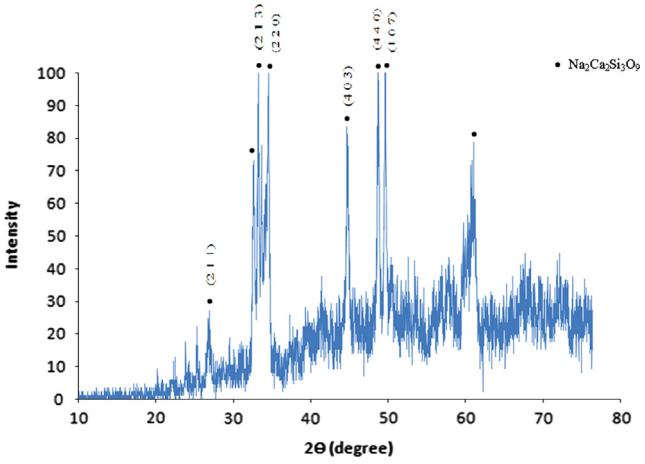

Fig. 2. XRD pattern of 45S5 bioglass sintered at 600 °C for 5 h.

Tafel slopes (β_a, β_c) were obtained from polarization curves by using the Tafel extrapolation method. Also, mean values and standard deviation was calculated. Polarization resistance (R_p) was calculated by Stern–Geary equation [20]:

$$R_P = \frac{\beta_\alpha \beta_c}{2.31_{corr}(\beta_\alpha + \beta_c)} \quad (1)$$

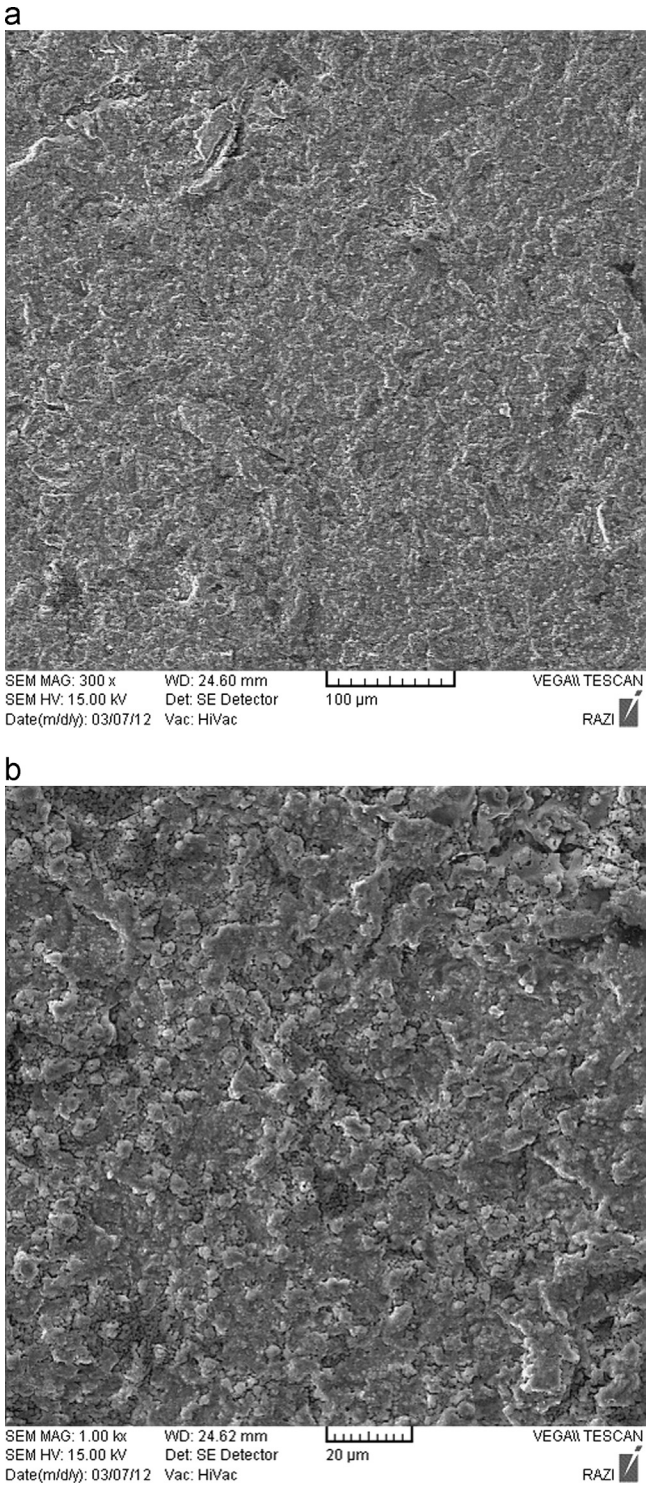

Fig. 3. SEM image of 45S5 bioglass- silica coat on 316L stainless steel; (a) X300; (b) X1000.

The bioactivity of coatings was investigated by soaking them in SBF solution at pH 7.4 [21] for 30 days at 37 °C (the composition of SBF solution is presented in Table 1) and the samples were analyzed by XRD, SEM/EDX (MIRA/TESCAN), potentiodynamic polarization experiments and the changes in SBF solution during immersion in SBF were studied by atomic absorption spectroscopy (AAS, GBC Avanta PM).

3. Results and discussion

3.1. Coating characterization

Fig. 1 shows XRD patterns of 45S5 bioglass before sintering and also after sintering at 600 and 700 °C for 1 h. Before sintering, $NaNO_3$ peaks are only identified and by sintering at 600 °C, although small amount of nitrates still remain, a crystalline phase starts to form which is identified as $Na_2Ca_2Si_3O_9$ (standard PDF #22-1455). By increasing sintering temperature to 700 °C, nitrates are completely removed; besides, the intensity of $Na_2Ca_2Si_3O_9$ crystalline phase increases and $Na_2Ca_3Si_6O_{16}$ (standard PDF #23-0671) appears as the second crystalline phase.

It is always desirable to lower the sintering temperature, because high sintering temperature causes phase changes in microstructure of substrate and lowers the mechanical properties [15]. Therefore, the samples were sintered at 600 °C for 5 h to achieve three aims of removing nitrates, decreasing the percentage of crystalline phases and lowering sintering temperature; the XRD pattern of this sample is shown in Fig. 2.

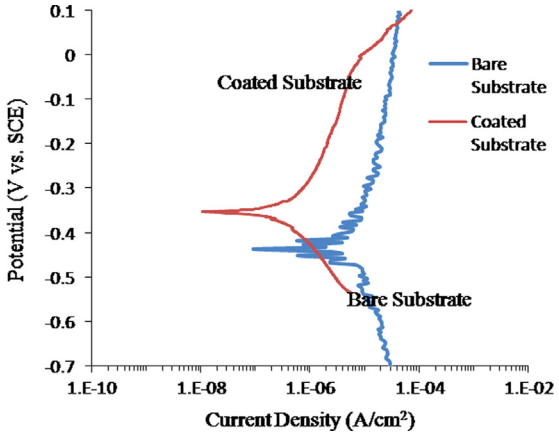

Fig. 4. potentiodynamic polarization curves for bare and 45S5 bioglass- silica coated 316L stainless steel in SBF at 37 °C after 1 h immersion.

Table 2
Mean values (standard deviation) of corrosion parameters according to potentiodynamic polarization tests for bare and bioglass- silica coated substrates soaked in SBF at 37 °C for 1 h.

Sample	E_{corr} (V versus SCE)	i_{corr} (nA/cm^2)	R_p (MΩ)
Bare substrate	-0.420 ± 0.002	1300 ± 75	0.14 ± 0.03
Silica-bioglass coated	-0.350 ± 0.002	35 ± 2	1.23 ± 0.07

As Fig. 2 shows, by increasing sintering time from 1 h to 5 h at 600 °C, the nitrate peaks are removed completely and even a diffusive background which is the indication of the amorphous phase is shown more clearly; besides, the $Na_2Ca_2Si_3O_9$ phase appears. Therefore, in this research, the coated samples were sintered at 600 °C for 5 h; because although the obtained samples have crystalline phase, the major part of them is amorphous and they are free from nitrates. Moreover, it must be said that $Na_2Ca_2Si_3O_9$ has been reported to have similar bioactivity to that of the glass phase [22] and calcium silicates and sodium–calcium silicates are frequently used as biomaterials and hence the development of these new phases is not expected to hinder the bioactivity of the 45S5 coatings [13].

The crystallite size of 45S5 bioglass sintered at 600 °C for 5 h is calculated from Scherer equation [23] which is approximately 50 nm.

An important parameter in dip coating procedure is surface preparation of substrates in order to prepare an adhesive and uniform coating without cracks. Adhesion results show that among different surface preparation used, coatings prepared on sandblasted substrates treated in nitric acid 25% vol for 12 h, had the best adhesion strength which was 5 MPa, while coatings prepared on sandblasted substrates and polished substrates had adhesive strength equal to 3 and 0.5 Mpa, respectively; these results are comparable with reported data [8,24].

For most coatings, the adhesive strength is because of mechanical interlocking and chemical bonding between the coating and the substrate [25,26]. By sandblasting, the surface roughness increases and as a result, the adhesion raises.

Fig. 3 shows SEM image of bioglass-silica coatings. Homogenous and crack-free coatings were obtained on 316L stainless steel substrate.

Fig. 4 shows the potentiodynamic polarization curves of bare and coated substrates in SBF at 37 °C. The corrosion current density (i_{corr}), corrosion potential (E_{corr}) and the corrosion resistance obtained from these curves are presented in Table 2. As Fig. 4 and Table 2 shows, 316L stainless steel corrodes rapidly in SBF in presence of chlorine ions, preferentially absorbed on its surface and the chlorine ions enhance ionization of the metal [27]. By using bioglass-silica coating on substrate, the corrosion potential becomes nobler and the corrosion current density decreases significantly.

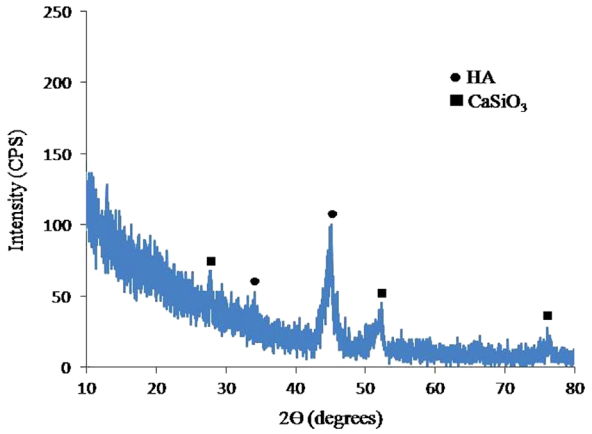

Fig. 6. XRD pattern of bioglass-silica coated samples after 30 days of immersion in SBF at 37 °C.

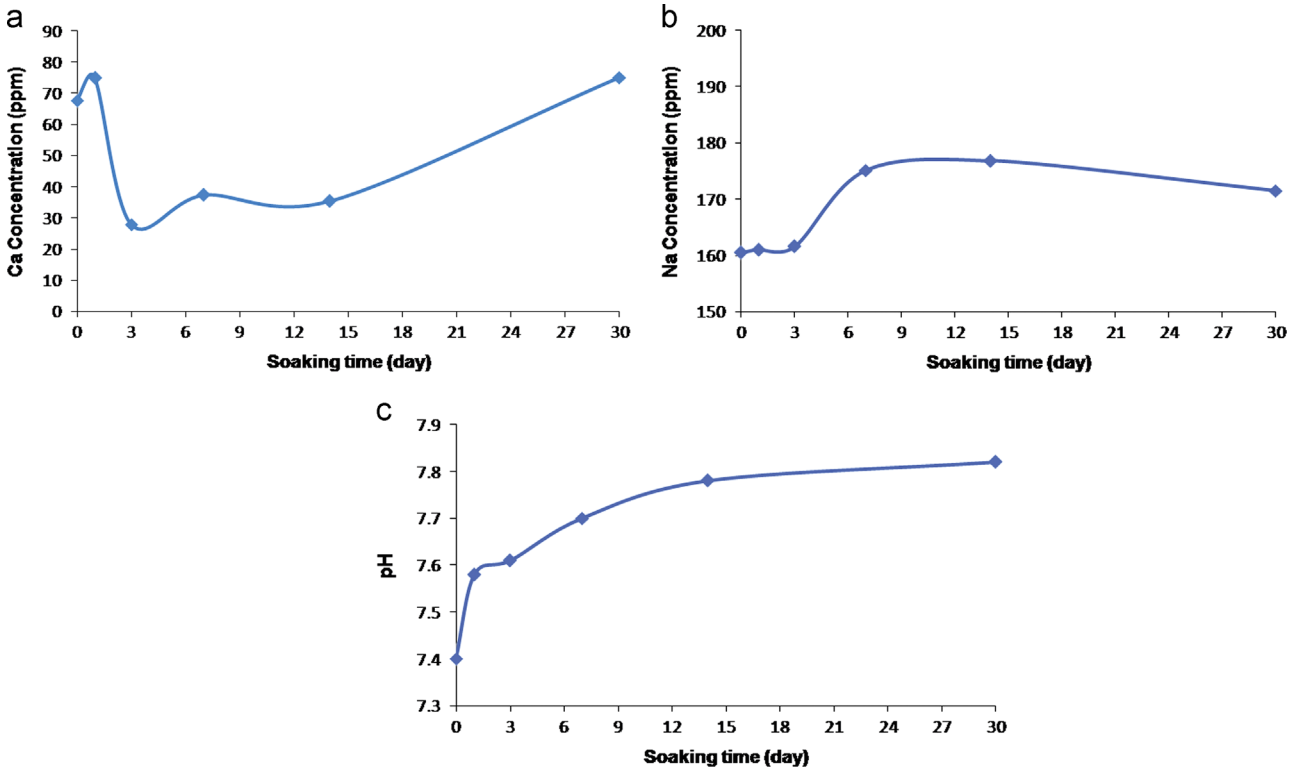

Fig. 5. variation of (a) Ca concentration, (b) Na concentration and (c) pH in SBF at 37 °C as a function of immersion time.

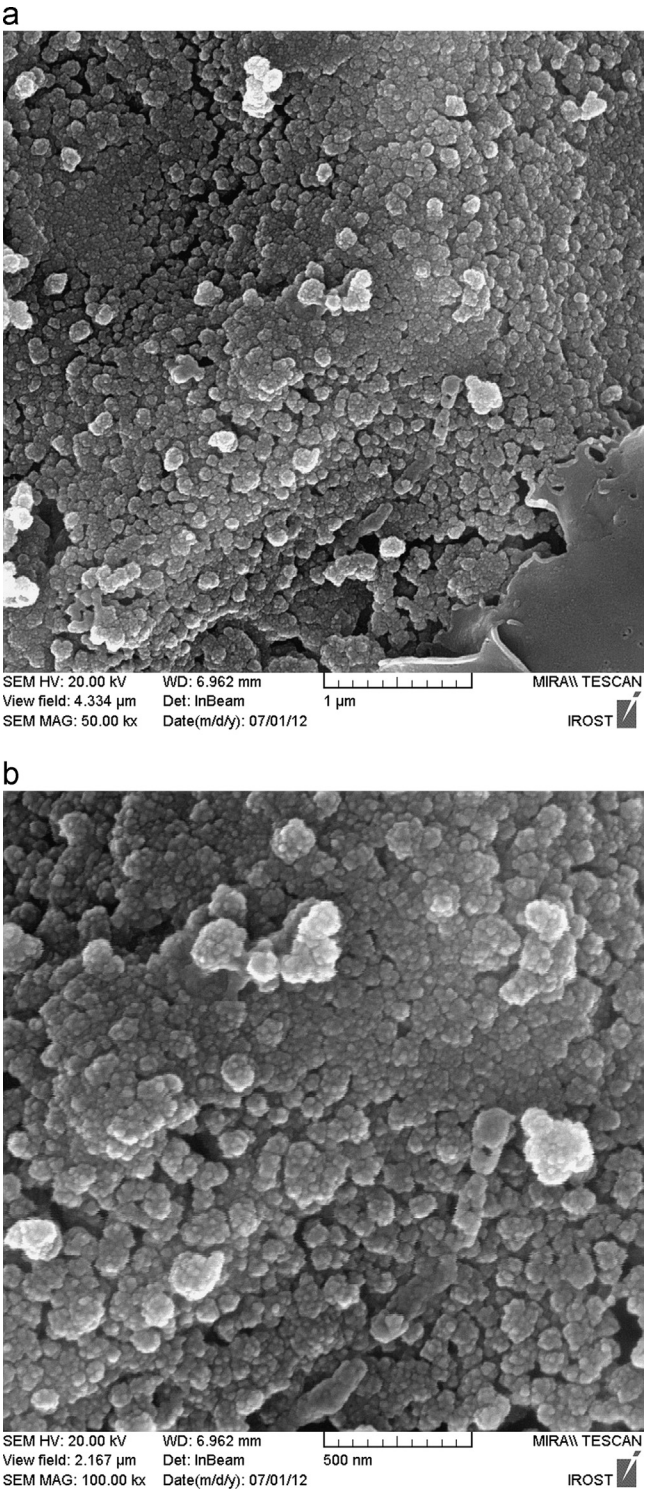

Fig. 7. SEM image of 45S5 bioglass-silica coated samples after 30 days soaking in SBF at 37 °C; (a) X50,000; (b) X100,000.

The corrosion behavior is essentially related to the morphology and defects of coated surface. The electrolyte infiltrates into the inner portion of the coating through the structural imperfections such as pores, cracks and pinholes existing in the coating and comes into contact with the deeper portion of the coating, causing corrosion [28]. The barrier effect of coatings is increased by the first SiO_2 coating that prevents the contact of electrolyte with the substrate after the dissolution of bioactive particles [29].

At the beginning of an interaction in a corrosive environment, the ceramic coating acts like a barrier between substrate and environment protecting substrate from corrosion. At overpotential conditions, coating layer scratches faster and then exposed areas increase; as a result, corrosion current increases. The diffusion of the oxidant ions speeds up and the corrosion rate increases due to debonding and elimination of the coating from the substrate [19]. Therefore, breakdown potential between bare and coated substrate differs.

3.2. Bioactivity

When bioglass reacts with SBF, both chemical and structural changes occur as a function of time within bioglass surface [4]. Fig. 5 shows the variation of Ca and Na concentration measured by atomic absorption spectroscopy (AAS) as well as pH values in the SBF solution versus immersion time.

Fig. 5(a) shows that, in the first day, Ca^{2+} concentration increases significantly and reaches to a maximum value which shows rapid Ca dissolution. Then, till the 3rd day, the Ca concentration decreases drastically. Since the Ca^{2+} concentration is controlled by both the release of Ca^{2+} from the coat to the SBF solution and the formation of phosphate or HCA on the coat. The decrease in the Ca^{2+} concentration in SBF is attributed to the rapid growth of the apatite nuclei formed on the surface of the glasses that overcame the release rate of calcium ions to the solution [30]. After that, the Ca^{2+} concentration again starts to increase gradually till the 30th day of soaking. The rise of Ca^{2+} concentration in SBF can be explained by the effect of the dense apatite layer which slowed the apatite growth.

Fig. 5(b) shows that the Na^+ concentration has increased gradually in the SBF and after 7 days of immersion, Na^+ concentration in solution becomes rather constant and only little changes take place.

Fig. 5(c) represents the pH changes in SBF solution during immersion test and it shows that the changes in pH during the first day of immersion is noticeable and pH increases from 7.4 to 7.58 after 24 h. Then, pH rises gradually and after 30 days, the value of pH increases up to 7.82. Increase in pH is result of ionic exchange between unstable cations like Na^+ and Ca^{2+} in bioglass coat with H^+ or H_3O^+ in media [31,32].

The observed behavior is consistent with mechanism of apatite formation similar to that described by Hench [4] for bioglass. Due to the release of Ca^{2+} and Na^+ into solution after immersion in SBF, silica network is attacked and this process is continued by formation of silanol (Si–OH) groups on surface, which are described by the following reactions [33,34]:

$$Si{-}O{-}Na^+ + H^+ + OH^- \rightarrow Si{-}OH + Na^+_{(solution)} + OH^- \quad (2)$$

$$2(Si{-}O)^{2-}Ca^{2+} + 2H_2O \rightarrow 2Si{-}OH + Ca^{2+} + 2OH^- \quad (3)$$

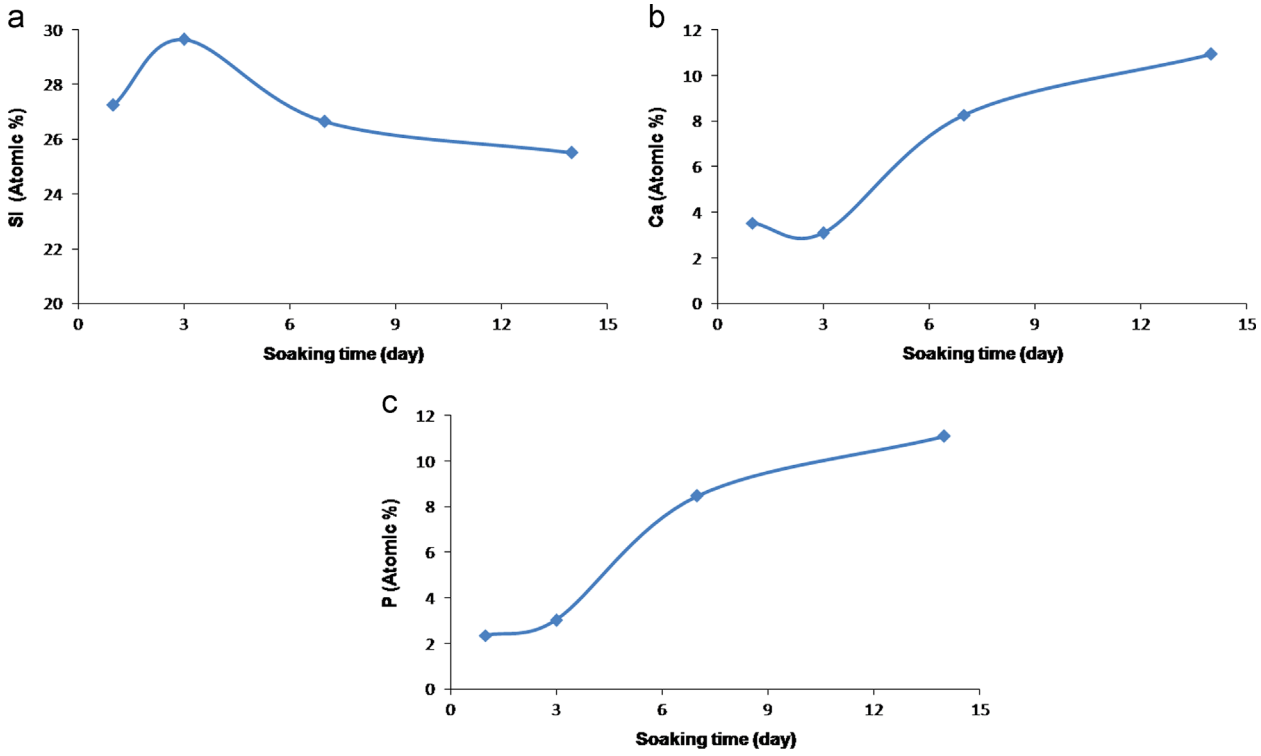

Fig. 8. changes in atomic percent of (a) Si, (b) Ca and (c) P on surface of coated samples versus soaking time in SBF at 37 °C, according to EDX analysis.

$$Si{-}O{-}Si + H_2O \rightarrow Si{-}OH + OH{-}Si \quad (4)$$

As mentioned, leaching of ions leads to an exposition of Si–OH network surface. This active surface stimulates deposition of calcium hydroxyapatite fine crystals on the bioactive glass surface which slowly reduces the area of exposed surface and therefore, the dissolution rate decreases [8].

Fig. 6 shows XRD pattern of coated samples after immersion in SBF for 30 days. In comparison with Fig. 2, after immersion in SBF for 30 days, the diffraction peaks of $Na_2Ca_2Si_3O_9$ phase disappear. In addition to decrease of crystallinity and increase of amorphous phase, diffraction peaks of hydroxyapatite (HA) and calcium silicate ($CaSiO_3$) appear.

In the sequence of interfacial reactions on the surface of bioglass in contact with body fluids, the bioactive glass first dissolves to form a silica-gel layer; then an amorphous calcium phosphate is formed from the hydrated silica-gel; and finally apatite crystallites nucleate and grow from the amorphous calcium phosphate [35]. Hence, according to Hench et al.'s theory, the amorphous phase detected by XRD after immersion in SBF could be the amorphous apatite and related amorphous calcium phosphates [18].

Fig. 7 shows SEM image of coatings after 30 days of immersion in SBF solution at 37 °C. It can be seen that after 30 days of soaking in SBF, the sample is fully covered by tiny spherical particles that according to XRD results, these spherical particles are apatite [17].

Fig. 8 presents EDX results for concentration changes of relevant elements occurred on the surface of coated samples during immersion in SBF. The Si and Ca fractions of all

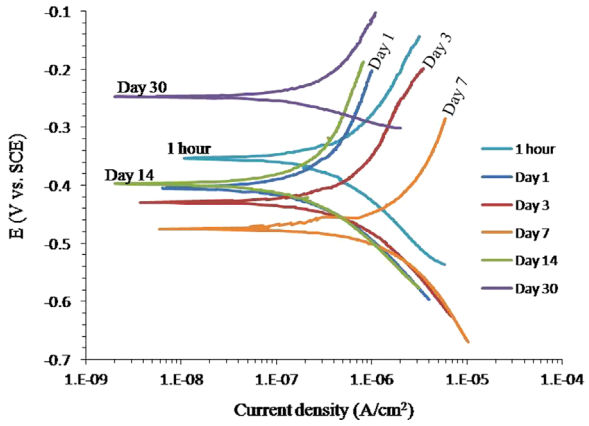

Fig. 9. potentiodynamic polarization curves of bioglass-silica coated samples after soaking in SBF at 37 °C for different immersion times.

samples begin to scatter during the first 3 days of soaking, indicating compositional heterogeneities [36]. After 3 days of immersion in SBF, all samples show an increase in the Ca and P contents and a decrease in silicon content, as expected, it is due to the formation of calcium phosphate layers, as observed by SEM. Moreover, this indicates the release of SiO_4^{2-} ions, which could be replaced by PO_4^{3-} [18].

It should be noted that the level of phosphorus and calcium was still lower than their standard amount in HA with theoretical composition of ($Ca_{10}(PO_4)_6$ $(OH)_2$). However, EDX analysis presents approximately the chemical composition of calcium phosphate film due to its penetration depth and the exact composition of the calcium phosphate layer cannot

Table 3
Mean Values (standard deviation) of electrochemical parameters according to potentiodynamic polarization tests for bioglass- silica coated substrates soaked in SBF at 37 °C for different immersion times.

Sample (soaking time)	E_{corr} (V versus SCE)	i_{corr} (nA/cm^2)	R_p (MΩ cm^2)	Porosity (%)
1 hour	-0.350 ± 0.002	35 ± 2	1.23 ± 0.07	8.5
1 day	-0.407 ± 0.002	13.7 ± 1	4 ± 0.12	3.4
3 day	-0.428 ± 0.002	16.1 ± 1	3.13 ± 0.09	4.5
7 day	-0.474 ± 0.002	27.2 ± 1	2.1 ± 0.07	6.1
14 day	-0.400 ± 0.002	4.5 ± 1	10.79 ± 0.15	1.2
30 day	-0.250 ± 0.002	1.8 ± 1	12.96 ± 0.17	0.7

be derived from the presented results. Also, this variation is expected as solution-mediated apatite formation and is dependent on several factors such as pH, temperature, initial Ca/P ratio and the presence of other inorganic ions [37].

Fig. 9 shows potentiodynamic polarization curves of bioglass-silica coated samples after immersion in SBF solution at 37 °C for different soaking times and the results obtained from this plot is presented in Table 3 and the coating porosity was estimated according to Eq. (5) [29]:

$$P = \frac{R_{ps}}{R_p} \times 10^{-\left|\frac{\Delta E_{corr}}{b_a}\right| \times 100} \quad (5)$$

where β_a is anodic Tafel slope, R_{ps} is the polarization resistance of the bare steel, R_p is the polarization resistance of the coated samples and ΔE_{corr} is the difference in corrosion potential between the coated and bare substrate [29].

According to Fig. 9 and Table 3, up until 7 days of immersion, corrosion current density increases from 13.7 ± 1 nA/cm^2 to 27.2 ± 1 nA/cm^2. Then, the corrosion current density starts to decrease till the 30th day that reaches to 1.8 ± 1 nA/cm^2. Moreover, the corrosion potential after the first day of immersion is -0.407 ± 0.002 V and it decreases to -0.474 ± 0.002 V after 7 days of immersion. Afterwards, the corrosion potential tends to become nobler and it reaches to -0.250 ± 0.002 V after 30 days of soaking.

Also, from the first day till the 7th day of immersion, polarization resistance decreases and the porosity percent increases; so, as mentioned, the corrosion current density increases and corrosion potential decreases. Then, the polarization resistance starts to increase and therefore, the porosity percent decrease after 30 days of soaking. So, the corrosion current density decreases significantly and the corrosion potential becomes more positive and tends to act nobler. Hence, the coatings show protective behavior.

In fact, after 7 days of exposure to SBF solution, the alkali and alkaline earth ions from the bioactive glass surface start to diffuse into the surrounding medium faster than ion precipitation on glass surface, leaving behind a corroded surface with increased surface area [8]; thus, the corrosion rate increases in the first days of immersion. Further, leaching of ions leads to an exposition of Si–OH networked surface. This active surface stimulates deposition of a thin film consisting of hydroxyapatite on the bioactive glass surface which slowly reduces the area of exposed surface [8] and pores and defects presented in the coatings could be blocked by corrosion products of the metal or by the degradation of the particles present in the coating [3]. This blocking could cause a higher resistance to the diffusion of the electro-active species to reach the metallic substrate increasing the apparent resistance of the system with time [27] and decreasing the rate of dissolution.

4. Conclusion

In this work, 45S5 bioglass-silica coatings were prepared on 316L stainless steel by sol–gel method. XRD patterns of 45S5 bioglass sintered at 600 °C for 5 h showed amorphous samples free from nitrates with small fracture of crystalline phase ($Na_2Ca_2Si_3O_9$) with crystallite size of 50 nm. Besides, the results confirmed that surface preparation of substrates had significant effect on coating properties. Bioglass-silica coatings exhibited a better electrochemical behavior in comparison with bare substrates. Further, in vitro behavior of coated substrates was considered during 30 days of immersion in SBF solution at 37 °C via XRD, SEM, AAS and potentiodynamic polarization tests that showed the growth of apatite and calcium silicates on the surface of coated samples.

References

[1] Raghuvir Singh, Narendra B. Dahotre, Corrosion degradation and prevention by surface modification of biometallic materials, Journal of Materials Science: Materials in Medicine 18 (2007) 725–751.
[2] A. Balamurugan, S. Rajeswari, G. Balossier, A.H.S. Rebelo, J.M. F. Ferreira, Corrosion aspects of metallic implants- An Overview, Materials and Corrosion 59 (11) (2008) 855–869.
[3] C. Garcıa, S. Cere, A. Duran, Bioactive coatings deposited on titanium alloys, Journal of Non-Crystalline Solids 352 (2006) 3488–3495.
[4] L.L. Hench, Bioceramics - from concept to clinic, Journal of American Ceramic Society 74 (7) (1991) 1487–1510.
[5] Masoud Mozafari, Fathollah Moztarzadeh, Mohammadreza Tahriri, Investigation of the physico-chemical reactivity of a mesoporous bioactive SiO2–CaO–P2O5 glass in simulated body fluid, Journal of Non-Crystalline Solids 356 (2010) 1470–1478.
[6] Alexander Hoppe, Nusret S. Güldal, Aldo R. Boccaccini, A review of the biological response to ionic dissolution products from bioactive glasses and glass-ceramics, Biomaterials 32 (11) (2011) 2757–2774.
[7] Marta Cerruti, David Greenspan, Kevin Powers, Effect of pH and ionic strength on the reactivity of Bioglasss 45S5, Biomaterials 26 (2005) 1665–1674.
[8] Chidambaram Soundrapandian, Sanghamitra Bharati, Debabrata Basu, Someswar Datta, Studies on novel bioactive glasses and bioactive glass–nano-Hap composites suitable for coating on metallic implants, Ceramics International 37 (2011) 759–769.
[9] J. Schrooten, J.A. Helsen, Adhesion of bioactive glass coating to Ti6Al4V oral implant, Biomaterials 21 (2000) 1461–1469.
[10] J. Schrooten, H. Van Oosterwyck, J. Vander Sloten, J.A. Helsen, Adhesion of new bioactive glass coating, Journal of Biomedical Materials Research 44 (1999) 243–252.
[11] Pablo Galliano, Juan Jose De Damborenea, M Jesus Pascual, Alicia Duran, Sol-gel coatings on 316L steel for clinical applications, Journal of Sol-Gel Science and Technology 13 (1998) 723–727.
[12] M.H. Fathi, A.Doost Mohammadi, Preparation and characterization of sol–gel bioactive glass coating for improvement of biocompatibility of human body implant, Materials Science and Engineering: A 474 (2008) 128–133.

[13] V. Cannillo, A. Sola, Different approaches to produce coatings with bioactive glasses: Enamelling vs. plasma spraying, Journal of the European Ceramic Society 30 (2010) 2031–2039.
[14] F. Pishbin, A. Simchi, M.P. Ryana, A.R. Boccaccini, A study of the electrophoretic deposition of Bioglass® suspensions using the Taguchi experimental design approach, Journal of the European Ceramic Society 30 (2010) 2963–2970.
[15] Bunyamin Aksakal.C. Hanyaloglu, Bioceramic dip-coating on Ti–6Al–4V and 316L SS implant Materials, Journal of Materials Science: Materials in Medicine 19 (2008) 2097–2104.
[16] Abdel Salam Hamdy, D.P. Butt, Environmentally compliant silica conversion coatings prepared by sol–gel method for aluminum alloys, Surface & Coatings Technology 201 (2006) 401–407.
[17] Renato Luiz Siqueira, Oscar Peitl, Edgar Dutra Zanotto, Gel-derived SiO2–CaO–Na2O–P2O5 bioactive powders: Synthesis and in vitro bioactivity, Journal of Materials Science and Engineering C 31 (2011) 983–991.
[18] Qi-Zhi Chen, Yuan Li, Li-Yu Jin, Julian M.W. Quinn, Paul A. Komesaroff, A new sol–gel process for producing Na2O-containing bioactive glass ceramics, Acta Biomaterialia 6 (2010) 4143–4153.
[19] G. Garbajal- de la Torre, M.A. Espinosa- Medina, A. Martinez- Villafane, J.G. Gonzalez- Rodriguez, V.M. Castano, Study of ceramic and hybrid coatings produced by the sol- gel method for corrosion protection, The open corrosion journal 2 (2009) 197–203.
[20] E.E. Stansbury, R.A. Buchanan, Fundamentals of electrochemical corrosion, ASM International246–254.
[21] Tadashi Kokubo, Hiroaki Takadama, How useful is SBF in predicting in vivo bone bioactivity?, Biomaterials 27 (2006) 2907–2915
[22] Yanfeng Xiao, Lei Song, Xiaoguang Liu, Yi Huang, Tao Huang, Yao Wu, Jiyong Chen, Fang Wu, Nanostructured bioactive glass–ceramic coatings deposited by the liquid precursor plasma spraying process, Applied Surface Science 257 (2011) 1898–1905.
[23] L. Lefebvre, J. Chevalier, L. Gremillard, R. Zenati, G. Thollet, D. Bernache-Assolant, A. Govin, Structural transformations of bioactive glass 45S5 with thermal treatments, Acta Materialia 55 (2007) 3305–3313.
[24] D.L. Wheeler, M.J. Montfort, S.W. Mc Loughlin, Differential healing response of bone adjacent to porous implants coated with hydroxyapatite and 45S5 bioactive glass, Journal of Biomedical Materials Research 55 (2001) 603–612.
[25] Mehdi Mazar Atabaki, Rabi'atuladawiyah Jafar, Jamaliah Idris, Sol-gel bioactive glass coating for improvement of biocompatible human body implant, Metalurgija 16 (2010) 149–163.
[26] Dean-Mo Liu, Quanzu Yang, Tom Troczynski, Sol–gel hydroxyapatite coatings on stainless steel substrates, Biomaterials 23 (2002) 691–698.
[27] L. Floroian, F. Sima, M. Florescu, M. Badea, A.C. Popescu, N. Serban, I. N. Mihailescu, Double layered nanostructured composite coatings with bioactive silicate glass and polymethilmethacrilate for biomimetic implant applications, Journal of Electroanalytical Chemistry 648 (2010) 111–118.
[28] C.C. Chen, T.H. Huang, C.T. Kao, S.J. Ding, Electrochemical study of the in vitro degradation of plasma-sprayed hydroxyapatite/bioactive glass composite coatings after heat treatment, Electrochimica Acta 50 (2004) 1023–1029.
[29] C. Garcıa, S. Cere, A. Duran, Bioactive coatings prepared by sol–gel on stainless steel 316L, Journal of Non-Crystalline Solids 348 (2004) 218–224.
[30] Na Li, Qing Jie, Sumin Zhu, Ruoding Wang, Preparation and characterization of macroporous sol–gel bioglass, Ceramics International 31 (2005) 641–646.
[31] P. Sepulveda, J.R. Jones, L.L. Hench, In vitro dissolution of melt-derived 45S5 and sol-gel derived 58S bioactive glasses, Journal of Biomedical Materials Research 61 (2002) 301–311.
[32] S. Lopez-Esteban, E. Saiz, S. Fujino, T.O ku, K. Suganuma, A.P. Tomsia, Bioactive glass coatings for orthopedic metallic implants, Journal of the European Ceramic Society 23 (2003) 2921–2930.
[33] Satadru Kashyap, Kyle Griep, John A. Nychka, Crystallization kinetics, mineralization and crack propagation in partially crystallized bioactive glass 45S5, Materials Science and Engineering C 31 (2011) 762–769.
[34] MariaVallet-Regi, C.Victoria Ragel, Antonio J. Salinas, Glasses with medical applications, European Journal of Inorganic Chemistry 6 (2003) 1029–1042.
[35] Qizhi Z. Chen, Ian D. Thompson, Aldo R. Boccaccini, 45S5 Bioglass-derived glass ceramic scaffolds for bone tissue engineering, Biomaterials 27 (2006) 2414–2425.
[36] Q.Z. Chen, K. Rezwan, D. Armitage, S.N. Nazhat, A.R. Boccaccini, The surface functionalization of 45S5 Bioglass-based glass-ceramic scaffolds and its impact on bioactivity, Journal of Materials Science: Materials in Medicine 17 (2006) 979–987.
[37] E. Kontonasaki, L. Papadopoulou, T. Zorba, E. Pavlidou, K. Paraskevopoulos, P. Koidis, Apatite formation on dental ceramics modified by a bioactive Glass, Journal of Oral Rehabilitation 30 (2003) 893–902.